

Performance Analysis of Adaptive Beamforming in a MIMO-millimeter Wave 5G Heterogeneous Wireless Network using Machine Learning

Sanjeev Chopra* and Ajay Kakkar
ECED, T.I.E.T., Punjab.
schopra_phd17@thapar.edu; ajay.kakkar@thapar.edu

Abstract

Beamforming (BF) always guides to determine the quality of received signal by an antenna array using Signal-to-Noise-Interference Ratio (SINR) in cellular base stations. This paper will help in the installation of 5G and 6G Millimeter-Wave (mm-Wave) heterogeneous wireless networks. Here, adaptive BF is designed and being implemented on the Machine Learning (ML) platform. The four ML methods having six BF properties to estimate the SINR of Multiple-Input-Multiple-Output (MIMO-mm-Wave) 5G wireless network are explored. The proposed algorithm suppresses noise plus interference and can reduce the power consumption. The python package pyArgus focusing on the BF and direction finding algorithms has been used for 20,000 simulations. The BF features namely noise variance, number of antenna elements, distance between antenna elements, azimuth angular range of receiving array, elevation angular range of receiving array and Direction of Arrival (DOA) of signal i.e. incident angle of Signal-of-Interest (SOI) are used in predicting the SINR. The 10-fold cross-validation experiment is performed to assess the robustness of the best predictive method. By conducting the rigorous simulations, it has been observed that Random Forest (RF) method outperforms over the three other ML methods such as Tree model i.e. rpart, Generalized Linear Model (glm) and Neural Network (nnet), which does the prediction inexpensive and faster. The

performance analysis parameters' result represents that the prediction of Mean Absolute Error (MAE) by RF is lowest 70.73 in value, and its Accuracy is maximum 86.40%, in value having the acceptable error on the training-testing data set.

Keywords: Adaptive Beamforming, Multiple-Input-Multiple-Output, Millimeter-Wave, 5G Machine Learning, Random Forest, Maximum Signal-to-Noise-Interference Ratio.

1 INTRODUCTION

BF is a smart antenna technique to provide a summation of the weighted signal over K users to produce the more concentrated transmitted signal from massive MIMO antenna arrays deployed in an mm-Wave 5G heterogeneous wireless network. It is rigorously used to distinguish real-time and nearly real-time data from other predicted data. It improves the link budget of mm-Wave and is used in sensor arrays of various fields such as radar, sonar, medical imaging, 5G vehicular communication systems and audio systems [2-3]. The mm-Wave communication needs a larger number of antennas at the transceiver to minimize the significant propagation path loss specifically by atmospheric absorption and to provide higher power gain in the form of BF. Moreover, hundreds or thousands of antennas can be accommodated at the transceiver due to the small carrier wavelengths at mm-Wave frequencies for a given size of antenna array, which provide the better flexibility of BF, but increase its complexity [4]. BF can be considered as a spatial linear filtering technique in 5G heterogeneous networks [5]. It gives MIMO diversity gain provided by coherent combining of multiple signal paths and in it, the radiation pattern of the antenna array is built in the direction of desired user while minimizing the interference for nearby users. The inter-cell interference are suppressed

using linear processing schemes in a coordinated BF fashion. The result of appropriate BF is that the links become isolated in direction, and intercellular interference plays a negligible role than in current small cellular networks. This fact implies that capacity gain in these systems is achieved by point-to-point technologies. Fixed BF is applied to the sources having fixed Angles- of-Arrival (AoAs). In adaptive BF, the weights of the array used are adapted to the changing signal environment in a continuous manner. The reliable Channel State Information (CSI) analysis is necessary in mm-Wave massive MIMO systems for near-optimal BF performance. However, acquiring this analysis becomes very cumbersome practically due to much variation in the used channel and the significant numbers of transceiver antenna elements. Since, in a currently smart antenna array structure having an interface as Digital Signal Processing (DSP), BF technique needs a fairly accurate estimate of DOA. High frequency (HF) communication signals received by the array are passed on to Receiver (RX) front end and then to Analog to Digital Converter (ADC) system. The DOA estimation algorithm is applied to analog to digital converted signal samples. The antenna array calculates and optimizes the BF weights so that the output beam will adapt itself to the DOA of SOI. Fig. 1 depicts the general block diagram of the smart antenna array system.

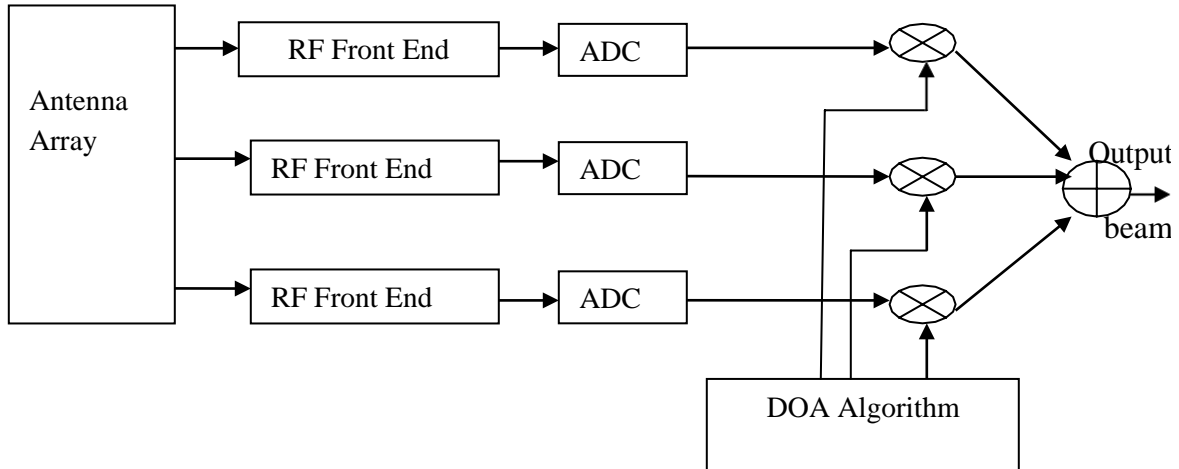


Fig. 1 - General Smart Antenna Array System

The MIMO capability includes several techniques, falling into the categories of BF, diversity, and spatial multiplexing. BF and diversity techniques can reduce the effects of multipath fading, which benefits other communications metrics. Spatial multiplexing can allow multiple independent, parallel data streams to be transmitted, increasing the overall throughput of a system. The availability of large bandwidth in mm-Wave range provides very high frequencies for 5G mobile communication networks as a promising candidate enabler. To tackle the signal propagation challenge through various paths, mm-Wave systems employ large antenna arrays that are expected to implement highly directional BF and provide higher link-level gains. BF with an antenna array of typically 64 to 512 elements per system within small form factors will reduce interference to adjacent users using a Multi-user (MU)-MIMO system and provides more directivity. In addition to more capacity in the MU-MIMO system, BF has other advantages like reduced energy consumption and the abundant mm-wave spectrum utilization. Its lower energy consumption brings a reduction in overall network operating costs by targeting individual user equipment's with their assigned signals. Full digital baseband precoding is not

preferred as it has extremely high hardware cost, space and energy utilization in a MIMO system, for the sake of the same number of Radio Frequency (RF) chains. The hybrid analog – digital precoding is a low-cost alternative solution to minimize the number of RF chains as it divides the precoding operations between the analog and digital domains [4, 6]. The digital weights of each RF chain are controlled in digital BF. The phase of the signal transmitted at each antenna is adjusted using analog phase shifters in analog BF. Therefore, the hardware-constrained mm-Wave massive MIMO communication system exploits both multiplexing gain and spatial diversity [4].

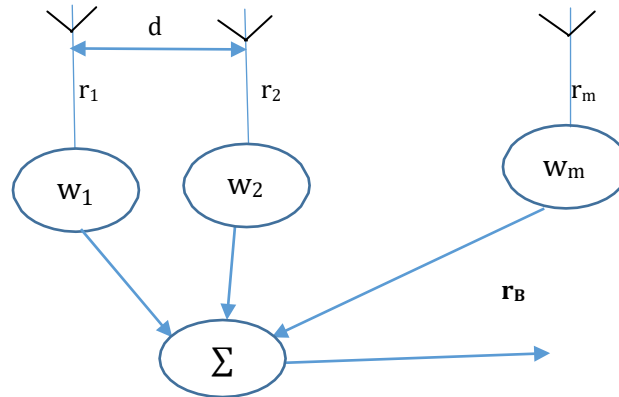


Fig. 2 - Working Principle of Beamformer

The BF adjusts the weights of the antenna elements of the array, which were employed adaptively to optimize the quality of signals under certain performance metrics [7]. From the fig. 2, the BF signal output is calculated using the following equation (1.1):

$$\mathbf{r}_B(\mathbf{t}) = \mathbf{w} \mathbf{H} \mathbf{r}(\mathbf{t}) \quad (1.1)$$

where $\mathbf{w} = [w_1 \dots w_M]^T$ corresponds to the vector of weights of the beamformer proportional to SINR, $\mathbf{r}(t)$ is the array output vector and \mathbf{H} is the channel matrix for a MIMO system described in equation (1.1). \mathbf{H} defines the complex channel gains between the antenna elements of the transmitter as well as of the receiver. It has dimensions $N_t \times N_r$, where N_t is the number of transmit antennas, and N_r is the number of receive antennas. Each value of \mathbf{H} represents the magnitude as well as phase of the channel gain between one pair of transmitter-receiver antenna elements. The matrix is reduced to a one-dimensional vector \mathbf{h} , where either a single antenna is assumed on one side of the system, or when the contributions from multiple antennas were combined, such as in the case of receiver diversity techniques, where only the totals at each receiver element are considered [8]. The Quality of Service (QoS) for the receive SNR is given by equation (1.2) which is as follows:

$$\text{QoS: (Normalized) Receive SNR} = |\mathbf{w}^T \mathbf{H}|^2 \quad (1.2)$$

where temporal variations of $\mathbf{H} \in \mathbb{C}^N$ are the realization of an underlying distribution, but in stochastic approximation case, the analysis of channel distribution is not required; rather most recent channel realization is used. This approximation is well suited for Frequency-Division Duplexing (FDD) systems.

For each receiver k , SINR is calculated using the equation (1.3) which is as follows:

$$\text{SINR} = \frac{|h_{jk}|^2 p_k}{\sum_{j=k} |h_{jk}|^2 p_k + \sigma^2} \quad (1.3)$$

where h_{jk} are the elements of the channel matrix \mathbf{H} , p_k is the power allocated to the k -th link, σ^2 is the noise power at the k -th receiver.

Related Work

The Multiple Signal Classification (MUSIC) technique, Estimation of Signal Parameters via Rotational Invariance Techniques (ESPRIT), and the Matrix Pencil method and its derivatives, were explained as a part of the BF technique to estimate the DOA of incoming signals based on the peaks of the spatial spectrum by Yang et al., 2010; Liao and Chan, 2011; Oumar et al., 2012; Chuang et al., 2015. However, the computational complexity of MUSIC and ESPRIT methods prevented them to be used in massive arrays. Several studies were done to classify BF techniques according to their physical characteristics especially. Gotsis and Sahalos in 2011 categorized BF techniques mainly as: switched BF and adaptive BF. Moreover, they classified these techniques into circular arrays, linear arrays, and rectangular arrays of array antennas. Hyper BF was categorized as either conventional (switched and fixed) BF or adaptive BF. Switched BF system [9, 10] enhanced SINR of the received signals by choosing one pattern from a lot of predefined patterns. The Butler matrix was developed by Butler and Ralph in 1961 as the most common solution for fixed BF. It depended on a switching network, which chose a suitable beam to obtain the desired signal from a specific terminal.

Various researchers such as Bae et al. in 2014, Huang and Pan in 2015, and Tiwari and Rao in 2015 discussed about the coverage area, interference suppression, capacity and complexity issues of switched BF and adaptive BF. Moreover, a beam typically served more than one Mobile Station (MS) [11]. Fixed BF used a fixed set of weights and time delays to combine the signals using the information mainly about the locations of the sensors in space and the wave direction of interest, received from the sensors employed in the array pattern [12]. Adaptive BF or phased array was based upon the maximization

of the desired signal at the main lobe provided by the maximum output SINR of beamformer and minimization of the interference signal [13-15]. It was observed that it was a flexible approach to find and estimate the SOI at the output of sensor array using data adaptive spatial or spatio-temporal filtering and interference cancellation. Its performance degradation could also take place, even if the SOI steering vector was precisely known, but the sample size during the training stage was small. Another reason for performance degradation was the environmental non-stationarities because of the fast variations of the propagation channel and rapid motion of interfering sources or antenna arrays. Fangxiao Jin et al. [16] proposed Maximum Correntropy Criterion (MCC) based vigorous cyclic array adaptive BF method to estimate DOA for cyclostationary signals to tackle against the Cycle Frequency Error (CFE) in impulsive noise as well as Gaussian noise environments. Practically, the impulsive noise often shows non-Gaussian properties. It was characterized by sudden bursts and frequently present in wireless systems [17, 18]. Due to this, a number of adaptive BF methods such as the Fractional Lower Order Moments-based Beamformer algorithms [19, 20], Linearly Constrained Minimum- 'Normalized Variance' based Beamformer algorithms [21, 22], MCC based Beamformer algorithms [23-25], and Correntropy based Beamformer [26, 27], were provided in the presence of impulsive noise. Taras Maksymyuk et al. discussed an iterative algorithm based on three neural networks for BF in a massive MIMO system, which required an intensive programming for its implementation [28]. Another classification of BF technique based on signal processing to increase the system capacity and performance was presented by Hur et al. in 2013 and Bogale and Le in 2014, wherein the researchers categorized the techniques into analog BF, digital BF, and hybrid BF. The

analog BF used the inexpensive phase shifters as a benefit for massive MIMO systems compared to digital BF, which has the advantage of providing a more accurate and speedy foundation results to obtain desired user signals. Vishnu V. Ratnam et al. discussed the use of Periodic Analog Channel Estimation (PACE) for designing RX beamformer in massive MIMO systems. In this technique, the channel estimates on one sub-carrier were used to perform BF on other sub-carriers and was found suitable for sparse channels with ≤ 10 multipath components in high SNR regime only. The suggested form did not support reception of multiple spatial data streams with more system mismatches. This technique had less loss in BF gain and a much lower CE overhead [29]. Kuo-Chen Ho et al. provided two weighted BF algorithms for low and high SNR regimes, which minimized the Symbol Error Rate (SER) for a given transmit power and the transmit power for a given SER. This technique of analog BF supported multiple spatial data transmission with few RF chains on the TX side in an mm-Wave channel model. This technique outperformed the conventional fully-digital zero-forcing BF scheme in terms of hardware cost and quantization effect noise [30]. However, digital BF suffers from high complexity and has an expensive design in massive MIMO systems. Hybrid BF was developed to obtain the advantages of analog as well as digital BF for massive MIMO systems and it employs small number of RF chains. Hybrid BF was classified as partially connected and fully connected. In fully connected type, additional components were used to combine RF signals and provide signal attenuation and power losses. On the other hand, partially connected type used the lesser RF chain access than number of antennas and led to serious drawbacks such as less directivity, wide beam-width and strong interference from other chains. To have a smaller beam-width,

interleaved partially connected array is used currently [31]. Mohammed A. Almagboul et al. proposed a partially connected hybrid BF inexpensive receiver based on Improved-Bat (I-BA) algorithm and robust adaptive beamformer in digital domain. I-BA was proposed to avoid the mismatch of DOA by adaptive beamformer and hence, to optimize its weights using the analog phase alignment by linear searching [32]. Hedi Khammari et al. provided an algorithm for allocating the resources as well as for designing the hybrid BF, and discussed K-mean unsupervised ML algorithm for optimal users grouping to reduce the feedback overhead. The proposed ML based analog BF along with zero-forcing digital precoding and user scheduling was used for better performance in terms of sum-rate [33]. Ahmet M. Elbir discussed the hybrid beamformer design in the mm-Wave - MIMO system. It used two Convolutional Neural Networks (CNNs) using the input of channel matrix based upon an optimization problem for the joint design of precoder and combiner. This technique utilized an algorithm for generating the training data for both networks [34]. Lorenzo Combi et al. designed an efficient algorithm for hybrid BF based on the matching-pursuit for a limited-size dictionary of analog beamformers, which was built on the statistical characteristics of the users' distribution. This dictionary was based upon the knowledge of spatial correlation of few DOAs and DODs representing the few radio front-haul channels at mm-Wave frequencies. Since the narrowband processing at the Resource Allocation Unit (RAU) was affected by the beam squint errors, the broadband analog processing with optical delay lines was adopted for HBF [35]. Susnata Mondal et al. demonstrated multi-band MIMO hybrid BF containing multi-antenna Carrier-Aggregation (CA), and RF (or hybrid) beamformer adaptation. This MMSE beam adaptation technique enabled the both main lobe and null adaption [36]. Linlin

Sun et al. proposed a robust hybrid analog-and-digital BF scheme containing Null Space Projection (NSP) in the analog BF domain and Digital Loading (DL) in digital BF domain to oppose DOA estimation errors at RX side [37]. Li Zhu et al. proposed the adaptive hybrid BF based on Dictionary Learning (DL) algorithm for an mm-Wave Line-of-Sight (LoS) MIMO communication system [38]. Yanan Liu et al. discussed the hotspot prediction and beam management for the adaptive Virtual Small Cells (VSCs) in 5G networks. The discussed deep learning technique improved both the cost efficiency and operational efficiency i.e. latency reduction of 5G networks and managed the beam of VSCs by the way of HBF [39]. Song Noh et al. designed a phase-shifted DFT method based multi-resolution HBF alignment sequence for channel sounding in large-scale mm-Wave - MIMO systems. This sequence designed a subset of codebooks used during the training period. This adaptive design system provided the good performance of average data rate by minimizing the training overhead in the considered mm-Wave systems [40]. Adaptive BF is inconvenient to implement, the major part of present studies related to massive MIMO systems tend to choose BF technique to fixed/switched BF due to its reliability for 5G requirements. A lot of researchers had implemented the various kinds of adaptive BF algorithms. However, virtually no study was available on adaptive BF in impulsive noise environments (i.e. low SINR) and other wide range of noise environments using ML to our best belief. Conventional feature- based approaches mainly depend upon the expert's knowledge, which may perform well on specialized solutions, but poor in generality and encounter high complexity and time- consuming. To solve these problems, ML classifiers were shown great advantages. Although ML methods have the advantage of solving classification problems efficiently and good

performance, the feature engineering still depends on expert experience to some extent, resulting in degradation of accuracy rate. Therefore, self-learning ability is very important in case of an unknown environment. Moreover, ML has a potential to solve the complex problems without explicit programming. Both the research community and industry have advocated the various applications of ML in the field of wireless communication for resource management such as beamformer design, due to its successful applications to many practical tasks like image recognition. To optimize beamformer vectors in a scenario of MIMO broadcast channel, the Weighted Minimum Mean Square Error (WMMSE) algorithm was designed, which transformed the weighted sum-rate maximization problem into a higher dimensional space to make the problem more tractable [41,42,43].

Problem Statement:

The suitable BF method increases the signal strength so that it may propagate a large distance through combining various scattered beam components into a single beam in a particular direction with the least affection of environmental conditions. The various researchers had worked on various BF methods, but no one tried to implement any of these methods on the ML platform. The novelty of the proposed work is that we are designing an adaptive or phased array BF system, and implementing as well as analyzing it on the ML platform.

Main Contributions of this paper:

1. The proposed algorithm is implemented on a ML platform and is analyzed by the four ML methods.

2. It works in Maximum Signal-to-Noise-Interference Ratio (MSINR) sense by the way of optimal adaptive BF and is capable of reducing power consumption as well as operational cost in a mm-Wave massive MIMO heterogeneous network by deploying suitable BF method.
3. The SINR responsible for the adaptive BF under a wide range of noise environments is predicted and maximized against target SINR using the various ML models.

The structure of this paper is as follows:

The introduction along with the related work is presented in section 1. The types, proposed work flowchart, and data set and methodology of BF are described in section 2. The subsections 2.1.1, 2.1.2 and 2.2 explain transmit BF using Maximum Ratio Transmission (MRT), transmit precoding for BF and proposed work flowchart of adaptive BF respectively. The considered data set and its features having qualitative assessment, and methodology used are presented in subsection 2.3. The subsection 2.3.1 describes the six relevant features required for the generation of target SINR. The ML methods and model evaluation are presented in section 3. The applicable four ML methods for the prediction of target SINR are discussed in subsection 3.1. Model evaluation using various performance analysis parameters is explained in the subsection 3.2. Section 4 explains simulation results and discussion. The subsection 4.1 is based upon the comparison of performance analysis parameters of the used ML methods. The subsection 4.2 discusses the results of validation and cross-validation simulation experiment. In the last, the conclusion is provided in section 5.

2 Types, Proposed Work Flowchart, Data Set and Methodology of

BF

2.1.1 Transmit BF using MRT

There are two methods for transmitting: the first is an adaptive technique called MRT and the second technique is precoding. The first technique uses the channel matrix between the transmitting and receiving antennas to optimize power at the receiver. The BF weighting matrix between a transmitter and a particular receiver antenna element, k [44], is defined by the equation (2.1) which is given as follows:

$$\mathbf{w}_k = \frac{\mathbf{h}_k^T}{|\mathbf{h}_k|} \quad (2.1)$$

where \mathbf{h}_k is the $N_t \times 1$ channel vector between the transmitting array and the receiver antenna. The quantity in the denominator is the absolute magnitude of the channel vector, which is the square root of the sum of the square magnitudes of each of the complex elements of the channel vector. This weighting matrix maximizes the beam to the specific receiver antenna, which is entirely based on the channel vector, scaling both magnitude and phase to form an optimal beam. This beam will likely not represent a specific direction in an environment with a great deal of multipath, and it may include multiple lobes taking advantage of the multipath for the specific transmitter-receiver element combination. When the receiver has more than one element, MRT was applied to form an optimal beam to the first element, and receiver diversity techniques were applied to further enhance the gain using the additional receiver elements.

2.1.2 Transmit Precoding for BF

This technique uses a precoding table to specify a collection of predefined beams. The model also provides a mechanism for defining a table of precoding weights that can be

applied to the H-matrix to perform transmit BF or diversity. The precoding weights provided by Alamouti and pseudo-Alamouti codes increased the probability that a receiver employing MIMO techniques will receive a signal with spatial diversity as an advantage. Precoding tables were used to define codebooks or collections of BF weights that can be used to support a BF method. When the precoding table is used to define multiple sets of precoding weights for each of a number of beams for a massive MIMO antenna array, it is attempted to use each set of weights and will select the set that provides the desired SINR. During a simulation, for each receiver, the model will attempt to use each beam and select the beam that provides the best SINR. This simulates a base station that has a fixed set of beams to choose from, which uses reference signals and feedback from each User Equipment (UE) to select the best beam for transmission to that UE.

2.2 Proposed Work Flowchart of adaptive BF

The BF technique is mainly used in radar and sonar systems. Its task is to adjust the array weights to maximize SINR in its output as the source moves, while maintaining a constant gain for the SOI. In BF array, noise and interference are minimized in the output and the beam pattern is optimized by the processor incorporated by adjusting the control weights with respect to a prescribed criterion. BF algorithms were based upon certain criteria like minimizing the variance, maximizing the SINR ratio, minimizing the Mean Square Error (MSE) [45-47], and were used to optimize the smart antenna patterns. The training of the network is performed and control weights are predicted from it in real time. To follow the significant users, 2-D arrays put null values in the direction of the interfering users [48]. The highly directional channel-aware BF supports long outdoor

links. The required RF chains are usually lesser to antenna elements. The number of available RF chains helps in the realization of a number of beams from a node per time instant. The required performance of a wireless system was achieved, if a beamformer was designed and algorithm alternatives were evaluated as the first step. In the next step, the beamformer was integrated into a system-level model and evaluated over a collection of parameter, steering, and channel combinations. The beam steering helps in a significant reduction of the delayed multipath components. Another cumbersome task is system level tradeoffs between performing BF in the RF domain and/or digital baseband domain. In the proposed work flowchart, an adaptive beamformer is designed with the aims of suppression of noise plus interference and reduction of power consumption. The propagation of mm-Wave is dominated by the LOS component. Hence, the knowledge of AoA of the wave is necessary for its reception at the RX. The optimal weight coefficients of array elements corresponding to all DOA's varying from $[-120^\circ; 120^\circ]$ are calculated/predicted in MSINR sense considering autocorrelation matrix of noise plus interferences and autocorrelation matrix of SOI. These autocorrelation matrices of noise and interferences are not correlated in nature. The necessary phase changes can be carried out with the various digital ICs available today in the market. The SOI autocorrelation matrix is generated by creating the array response vector for SOI. This adaptive algorithm is used for optimal BF in massive MIMO mm-Wave systems and is capable of reducing power consumption by deploying the suitable BF method. The proposed work flowchart of adaptive BF as shown in fig. 3 is as follows:

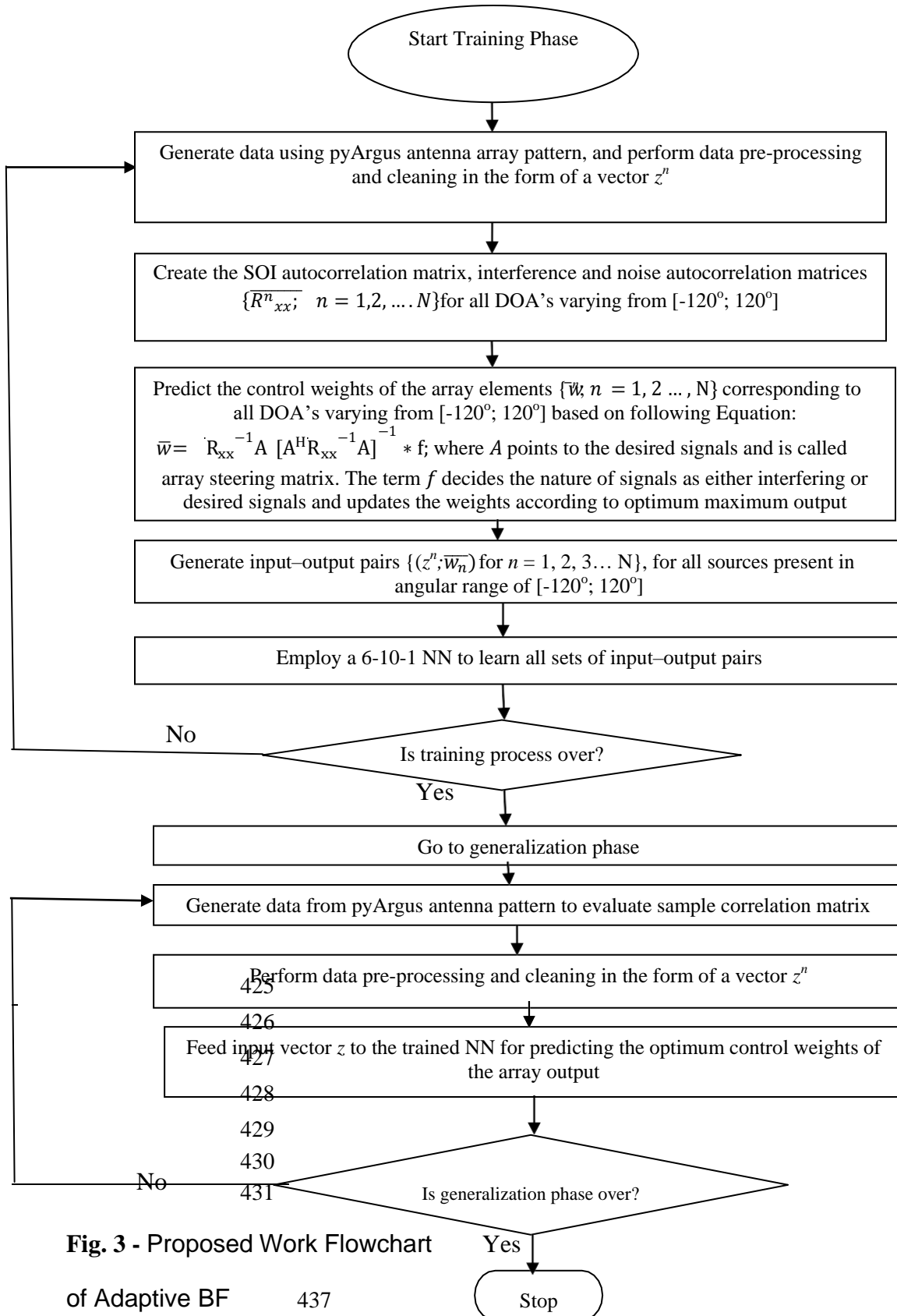


Fig. 3 - Proposed Work Flowchart of Adaptive BF

2.3 Data Set and Methodology

2.3.1 Data set and its features having qualitative assessment

The required data is generated for the work using modeling and simulation. The python package pyArgus [1] has been used for 20,000 simulations. The noise variance, Pnoise is between 0.001 and 0.1, both are inclusive; N is the number of elements of an antenna lying between 2 and 10, both are inclusive; d is the distance between the consecutive antenna elements measured in λ and lying randomly between 0 and 1(inclusive); a and b are azimuth and elevation angular ranges of receiving array respectively each lying between -120° and $+120^\circ$, both are inclusive; Theta_soi is SOI lying between -120° and $+120^\circ$, both are inclusive. The values of a and b provide a help in the generation of incident angles of interferences. Table 1 shows a brief description of the features, namely as Pnoise, N, d, a, b and Theta_soi using RF in terms of % Inc MSE and Inc Node Purity used for the generation of BF beam in this study. The higher value of any feature plays a more significant role in the generation of BF beams. Table 2 describes the sample dataset used containing the randomly selected values of all six features. The modeled entries are simulation of python-based signal processing algorithms applicable in antenna arrays (pyArgus).

Table 1 Description of the features using RF

Feature	Information (% Inc MSE)	Inc Node Purity
P _{noise}	148.12	1672223101
N	72.72	315851000
d	39.68	138440244
a	0.74	112363333
b	8.24	115403801
Theta_soi	10.49	134960829

Table 2 Sample dataset

P_{noise}	d	N	theta_soi	a	b	SINR
0.053	0.3	10	-102	117	-62	188.63
0.018	0.2	10	4	-8	-10	2.17
0.028	0.9	2	-67	-89	-31	67.05
0.016	0.5	3	48	-96	-5	101.77
0.094	0.1	8	84	117	35	59.91
0.071	0.4	4	96	21	33	52.31
0.09	0.9	8	102	-14	94	88.89
0.033	0.8	10	-32	-81	10	300.77
0.023	0.7	2	-61	-10	-18	63.82
0.058	0.4	8	-60	-73	-89	131.47
0.091	0.8	8	-75	-70	14	86.53
0.061	0.6	9	-77	10	-4	147.06
0.027	0.2	6	8	-87	-98	210.54
0.007	0.6	5	27	-9	47	549.88
0.042	0.7	3	-90	17	61	71.40
0.051	0.7	3	120	-46	-65	58.52
0.095	0.4	2	-1	-111	-30	1.52
0.042	0.5	4	-120	-107	53	93.08
0.07	0.7	3	61	-81	37	34.01

2.3.2 Methodology used

The methodology of the proposed system, which is used for predicting the target SINR in terms of model evaluation parameters, consists of six steps. These steps as mentioned in Fig. 4 are described as follows:

In step 1, the data is collected through modeling and simulation, and its pre-processing and cleaning is carried out to enhance its accuracy, validity, completeness, consistency and uniformity in step 2. The step 3 consists of finding the features of importance as mentioned in table 1 of subsection 2.3.1, required to decide their role in the generation of BF beam. In step 4, a model building is done on the pre-processed and cleaned dataset. The step 5 consists of evaluation of the built model using 4 ML methods in terms of performance analysis parameters as mentioned in the table 4 obtained using the equations (3.2) – (3.4) of sub-section 3.2. In step 6, the result is analyzed by the validation and cross-validation simulation experiment as mentioned in sub-section 4.2.

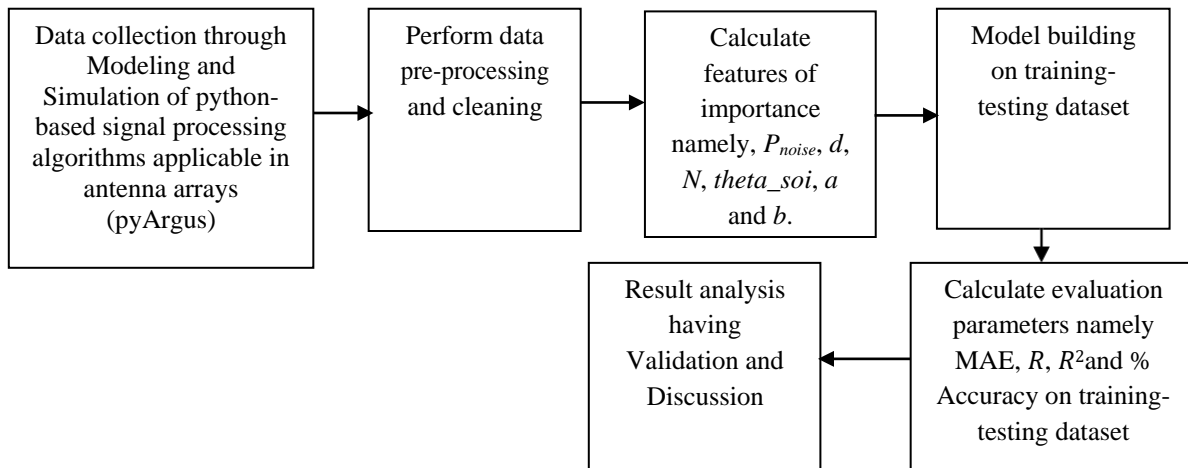


Fig. 4 - Various Steps of Methodology used

3 ML Methods and Model Evaluation

3.1 Machine Learning (ML) Methods

The four ML methods (shown in Table 3) used for prediction of SINR of the received signal are present in R open source software, which is licensed under GNU GPL.

Table 3 ML methods used

Model	Method	Package	Tuning Parameters and associated Values measured
Decision Tree [49]	rpart	rpart	minSplit=20, maxDepth=3, minBucket=7, n=14000
Random Forest [50]	RF	randomForest	$N_{tree}=500$, $m_{try}=2$
LM [51]	lm	glm	none
NN [52]	neuralnet	nnet	$h_{layers}=10$, $maxNwts.=87$, $maxit=20000$

A lot of ML methods are available, but only four methods, namely as rpart, RF, lm and neuralnet are applicable because the proposed model supports only regression and classification data, and output of the proposed model is a numeric value. These methods are explained briefly as:

(a) Decision Tree (rpart): This method is an extension of C4.5 classification algorithms described by Quinlan [49]. It does not support online learning and suffers from easy overfitting problem. Therefore, it is not well suited for the proposed model.

(b) Random Forest (randomForest): It depends upon a dense collection of trees using the inputs of random nature [50]. It supports both types of regression and classification problems having large data sets. It also helps in the identification of most significant

variables from hundreds of input variables. It is scalable in nature to any number of dimensions and has generally quite acceptable performances. N_{tree} and m_{try} are the number of trees and number of variables tried at each split, respectively.

(c) Linear Model (glm): It carries out regression, single stratum analysis of variance and analysis of covariance [51].

(d) Neural Network (nnet): Training of neural network is done using back-propagation, resilient back-propagation with or without weight or the modified globally convergent version [52]. The neural network accepts the weights of connections between neurons. When all weights are trained, it is used to predict the class or quantity. h_{layers} , $maxNwts$, and $maxit$ are the number of hidden layers, maximum network weights and maximum number of iterations, respectively. The neuralnet used is 6-10-1 network. The tuning parameters used in each method minimize the error.

3.2 Model Evaluation

Adaptive beamformers are evaluated in terms of the beamformer response, the output SINR, the array gain, the array sensitivity, and the white noise gain.

The output SINR is determined by the equation (3.1) which is as follows:

$$\mathbf{SINR} = (\mathbf{w}^H \mathbf{R}_{SS} \mathbf{w}) / (\mathbf{w}^H \mathbf{R}_{(i+n)} \mathbf{w}) \quad (3.1)$$

where \mathbf{R}_{SS} is sample covariance matrix of the source observed at the array beamformer, \mathbf{R}_{i+n} is the covariance matrix of the interference and noise considered together. The adaptive beamformer is evaluated by the output SINR only, which provides a measure of the quality of communication, and estimates the ratio between the SOI and noise plus interference. It is optimized under wide range of noise environments by optimizing the value of spacing between elements, element tapering, lattice structure between elements

and increasing the number of elements in antenna array used. The BF model is evaluated in terms of the following 4 performance analysis parameters given by equations (3.2) – (3.4) [53], which are not derived here:

3.2.1 Mean Absolute Error (MAE)

It measures the error rate of a regression model. However, it can only be compared between models having errors in the same units [53]. It is calculated by the equation (3.2):

MAE = Average of Absolute value

$$(\mathbf{p}_i - \mathbf{a}_i) \text{ for } \mathbf{n} \text{ number of iterations} \quad (3.2)$$

where a_i is i^{th} actual SINR target value and p_i is i^{th} predicted SINR target value. It is calculated for all ML methods, which are shown in table 4.

3.2.1 Correlation (R)

It provides the statistical relationships between true and predicted values. It is defined by the equation (3.3):

$$\mathbf{R} = \frac{\sum_{i=1}^n (x - \bar{x})(y - \bar{y})}{\sqrt{\sum_{i=1}^n (x - \bar{x})^2 \sum_{i=1}^n (y - \bar{y})^2}} \quad (3.3)$$

where x is the true value, y is the predicted value, \bar{x} is the average of the all true values, \bar{y} is the average of the all predicted values and n is the number of iterations. Correlation is present between 0 and 1, and is considered as good if its value approaches 1[53]. It is calculated for all ML methods, which are shown in table 4.

3.2.3 Coefficient of Determination (R^2)

It evaluates the proportion of variance of the dependent variable, provided by the regression model and provides its explanatory power [53]. For perfectness of the model R^2 is 1, and for its failure, R^2 is zero. It is calculated by taking the square of the R – value between the predicted and observed values for all ML methods, which are shown in table 4.

3.3.4 Accuracy

Training Loss and accuracy give overall measures of the model's performance. The accuracy is improved by preprocessing the data. It is calculated by the following equation (3.4) as percentage deviation of predicted target with true target with some acceptable error:

$$\text{Accuracy} = \frac{100}{n} \sum_{i=1}^n q_i \quad (3.4)$$

$$q_i = \{1 \text{ if } \text{abs}(a_i - p_i) \leq e$$

$$0 \text{ elsewhere,}$$

where a is the true target, p is the predicted target, n is the total number of iterations and e is the acceptable error [53]. It is calculated for all ML methods, which are shown in table 4.

3.2.5 K-Fold Cross Validation

It measures the robustness of the predictive method employed. The generated dataset is randomly divided into say k equal size subsamples as a first step. Thereafter, out of the

k Sub-samples, a single subsample is retained as the validation data for testing the method, and the remaining $k - 1$ subsamples are used for carrying out the training of the generated data. The cross-validation process is then repeated K-fold of times, with each of the k subsamples used exactly once as the validation data. Then, all the results from K-folds can be averaged to provide a single estimation. The 10-fold validation and cross-validation in terms of true and predicted values of target SINR are shown in figs. 7 and 8.

4 Simulation Results and Discussion

The proposed adaptive BF system is hybrid in a sense that it is a combination of an analog part driven by a computer controlled system and a ML part. The prediction results of all employed ML methods on the training-testing data set are analyzed. All the models, which were discussed in section 4, have been run on a sample dataset (shown in Table 2) and evaluated on correlation, R^2 , MAE and % accuracy. The dataset is handling a smaller number of input features, which are larger in observation values. The 10-fold validation is used to assess the robustness of the best predictive method. The regression model suffers from overfitting problem as the criterion used for its training is not exactly the same as the criterion used to judge its efficacy. So, the validation experiment has been conducted on the generated dataset using best predictive model selected from training-testing experiment. The overfitting issue may have less chance, if the number of parameters in the employed network is much smaller as compared to the total number of data points in the training set. If the size of the training dataset is increased by collecting more data, techniques like regularization and early stopping are not feasible to prevent over-fitting.

4.1 Training-Testing Simulation Experiment

The generated data set is divided into two sets - one set is used for training first and thereafter; the second set is used to test the performance of the result. The generated data set is distributed to 70% and 30% respectively for all employed methods in training-testing experiment. Table 4 depicts the comparative performance of all used methods in the prediction of SINR on correlation, R^2 , MAE and % accuracy. The performance results as shown in figs. 5 and 6 shows that RF method outperforms over the other three ML methods employed in the prediction of target SINR as there is the closer; more positive and linear relationship between true and predicted values as compared to other three ML models. Fig. 5 (b) and fig. 6 (b) depicts the scatter plot between predicted value and observed value of target SINR on training and testing dataset respectively using the best RF model. The SINR of the received signal can be increased by BF technique.

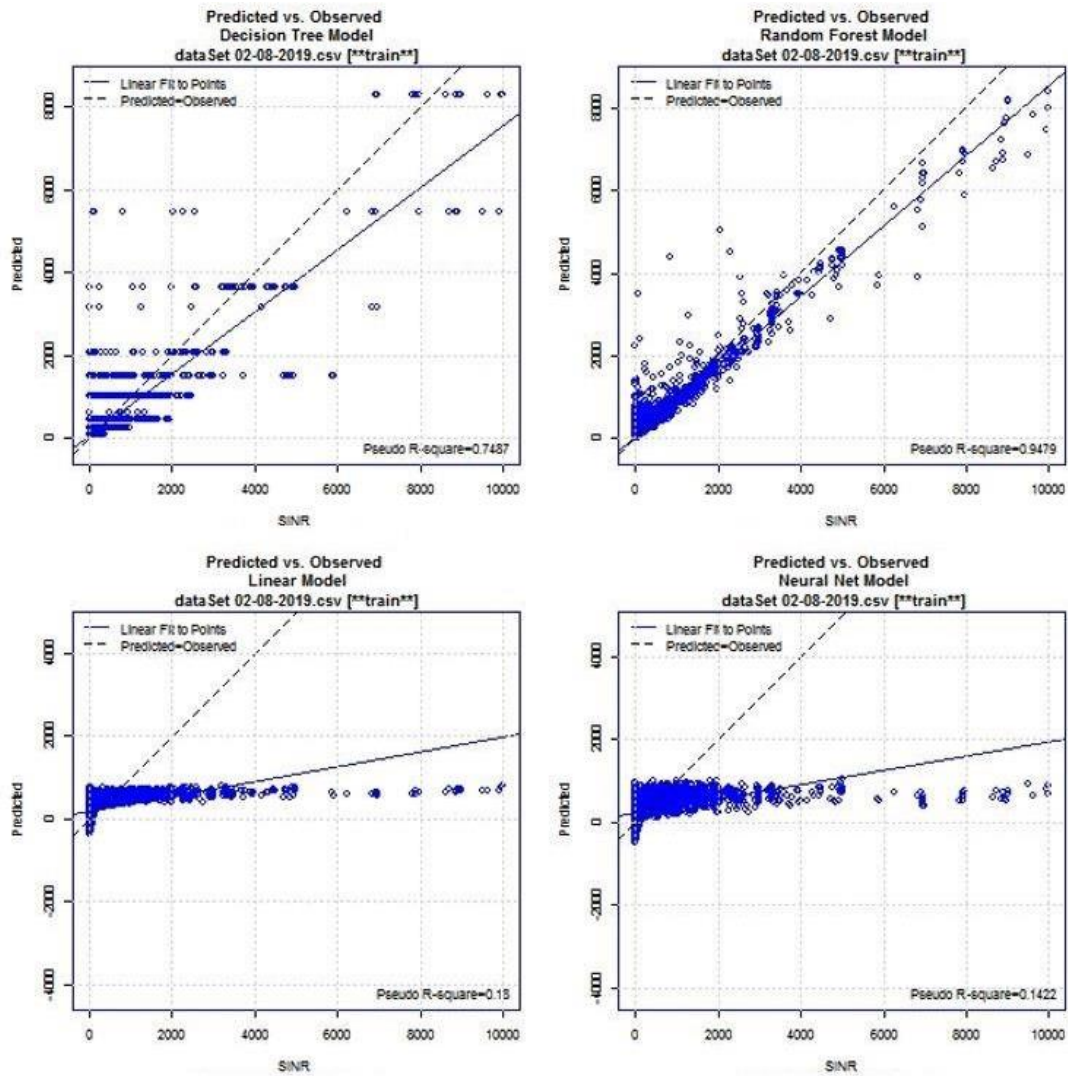


Fig. 5 (a) Predicted vs. Observed Decision Tree Model (b) Predicted vs. Observed Random Forest Model (c) Predicted vs. Observed Linear Model (d) Predicted vs. Observed Neural Net Model on Training dataset

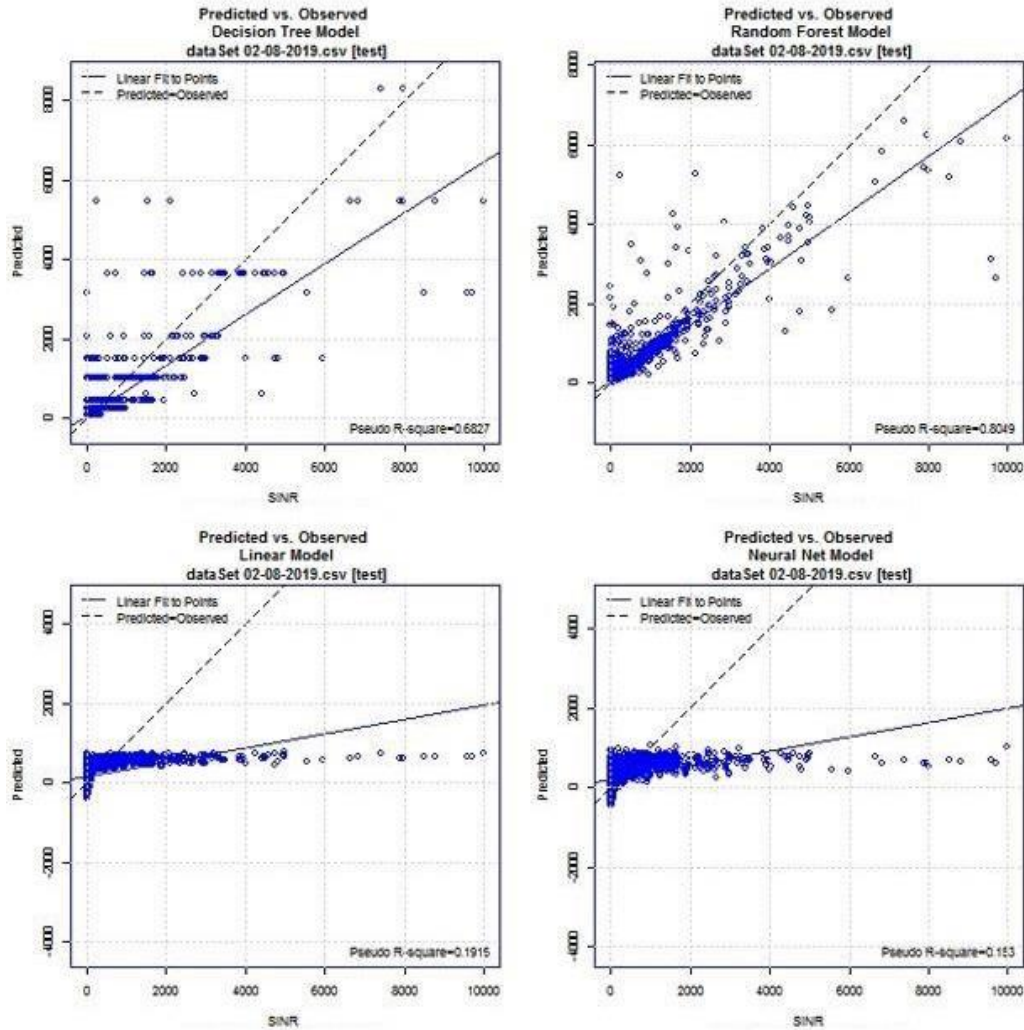


Fig. 6 (a) Predicted vs. Observed Decision Tree Model (b) Predicted vs. Observed Random Forest Model (c) Predicted vs. Observed Linear Model (d) Predicted vs. Observed Neural Net Model on Testing dataset

Table 4 Performance comparison of employed ML methods as shown in table 3 in the prediction of R, R², MAE and % Accuracy on training-testing dataset

Model used	Performance Analysis Parameters			
	R	R ²	MAE	% Accuracy
Decision Tree [49]	0.87	0.76	122.52	72.97
Random Forest [50]	0.92	0.85	70.73	86.40
LM [51]	0.42	0.18	208.18	36.12
NN [52]	0.20	0.04	211.53	42.50

The MAE is used to measure the average of absolute values of difference values between predicted and true values. It is computed using equation (3.2) and Table 4 depicts the MAE of four employed methods. It has been found that the RF model has the lowest MAE of 70.73 as compared to the other three models on the training-testing dataset. The R value is computed using equation (3.3) and Table 4 presents the R value of the employed methods. It has been observed that the RF model has the largest R value of 0.92. The R² parameter is computed by taking the square of correlation and Table 4 presents the R² parameter of the employed methods. It has been found that the RF model has the largest R² of 0.85 in the prediction of target SINR on the training-testing dataset. Accuracy is computed using equation (3.4) with some acceptable error and Table 4 depicts the % accuracy of the employed methods. It has been observed that the RF model has the largest accuracy of 86.40% having acceptable error in the prediction of target SINR on the training-testing dataset.

Table 5 Comparison of BF results based on ML of various researchers and our paper

Paper/ Author(s)	[49]/J. R. Quinlan (1986)	[53] / Prashant Singh Rana et al. (2014)	[34] Ahmet M. Elbir (2019)	[54] Francisco Hugo Costa Neto et al. (2019)	[55] Hyung Jun Kwon et al. (2019)	Results of the proposed work	Salient remarks
Type of model/Essential Simulation Conditions/ Parameter(s)							
Type of Model used	Complex decision tree	ML based modeled protein structure which was based on RMSED- prediction model	CNN based frame work	The downlink of a massive- MIMO system	ML model	Using the best RF model, the proposed work is having the following performan ce analysis parameters :	1. The dataset of paper [53] is little bit more correlated in nature, but its accuracy is much lower than the accuracy of the proposed work.
Essential Simulation Conditions/ Attributes used	Outlook, temperature, humidity and windy at 100%	Physicoche mical properties	$N_R = N_T = 36,$ $N_S = 3,$ Uniform square arrays with 0.5λ spacing, $N^{RF} = N^{RE} =$ $4,$ <i>No. of realizations of</i>	Angle sector= 60° , BS height=10 m, UE height=1.5 m, UE track=linear, UEs speed=3 km/h, BS antenna model = (3GPP)-	having 17 input nodes, M hidden layers with N hidden nodes and	Correlation - 0.92, R^2 - 0.85,	

		noise		<i>channel matrices, N = No. of noisy channel matrices, L = 100, all transmit and receive azimuth and elevation angles which were uniform randomly selected from the interval $[-60^{\circ}, 60^{\circ}]$ and $[-20^{\circ}, 20^{\circ}]$ respectively</i>	mm-Wave, BS vertical antennas=8, BS horizontal antennas=8, BS element array spacing=0.5 λ m, UE antenna model=omni, UE antennas=1, no. of simulation rounds=50	4 output nodes	Mean Absolute Error-70.73 and % Accuracy-86.40, as shown in table 4.	2. The accuracy of the proposed method mainly depends upon the type of the problem considered, and a way of dataset collected and its features of importance.
Parameters Measured by various researchers	Error rate (%)	Error rate of all attribute s= 25.9%	Not considered	Not considered	Not considered	Not considered		3. No other researcher had considered all ML methods as well as no researcher had implemented the designed BF algorithm on ML platform.
	Accuracy (%)	Not considered	RMSED based 78.82 %	Not considered	Not considered	Not considered		

Spectral efficiency (bits/s/ Hz)	Not considered	Not considered	(5 - 40) of HBF (Deep Learning) DL vs. SNR (-20 - 20) dB	Not considered	Not considered
NMSE	Not considered	Not considered	Not considered	(approx. 10-2.5 - less than 10-4) of the estimated channel vector for pilot sequence length =128 vs. SNR (0 - 20) dB of the beam	Not considered
Sum rate	Not considered	Not considered	Not considered	Not considered	(2 - approx. 15) of the TXs for 1000000 samples vs. SNR (0 - 25) dB

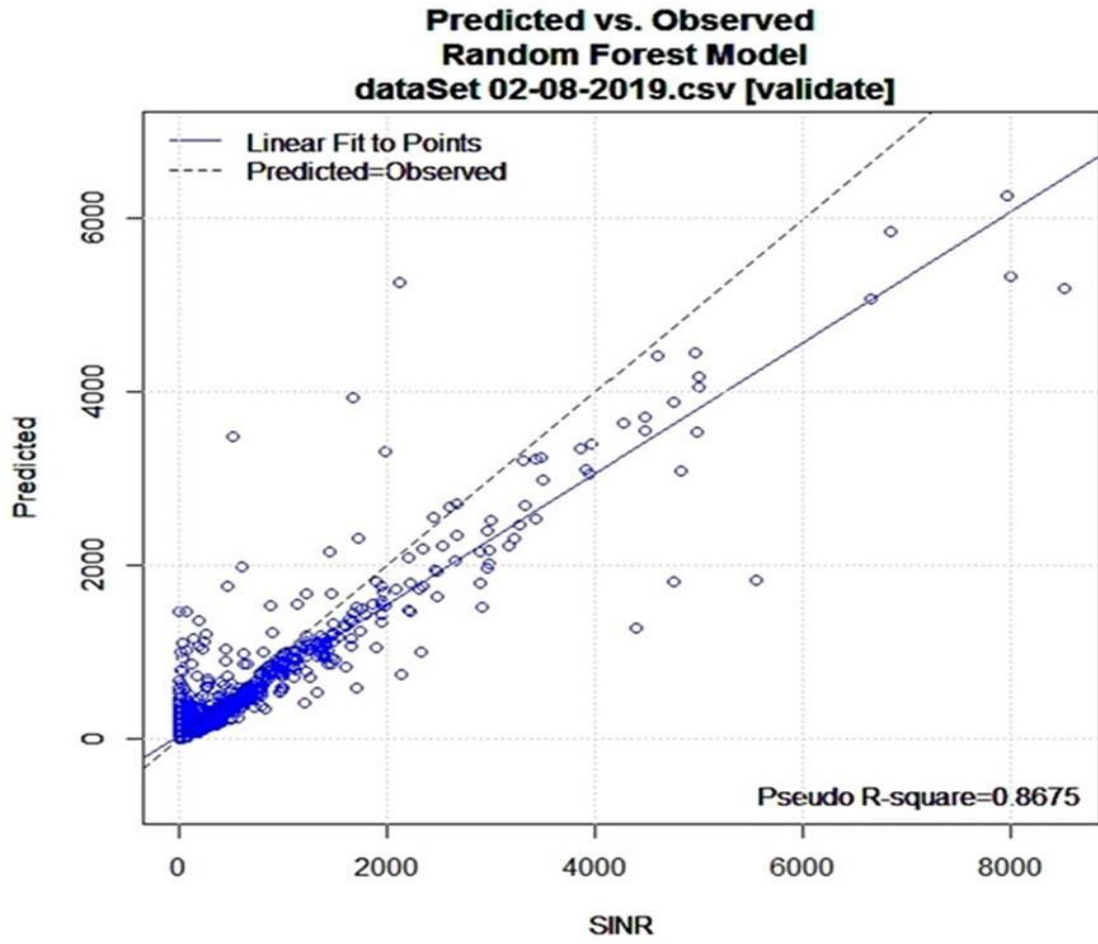
679 Our accuracy result is better than the Root Mean Square Deviation (RMSD) - based result as
680 shown in table 5 having the acceptable error on the training-testing data set of the research paper
681 [53]. The electronically steered BF applied and the corresponding results obtained as shown in
682 tables 4 and 5 play an important role in BS antennas providing the super-high spectrum efficiency
683 through spatial multiplexing, data rate, energy efficiency, network capacity and throughput for
684 near-instant and full unlimited connectivity human-like intelligent 6G wireless networks. The
685 network throughput can be increased by providing hundreds of beams serving a large number of
686 users at the same time in the form of massive-user MIMO in future 6G wireless networks.

687 *4.2 Validation and Cross-Validation Simulation Experiment*

688

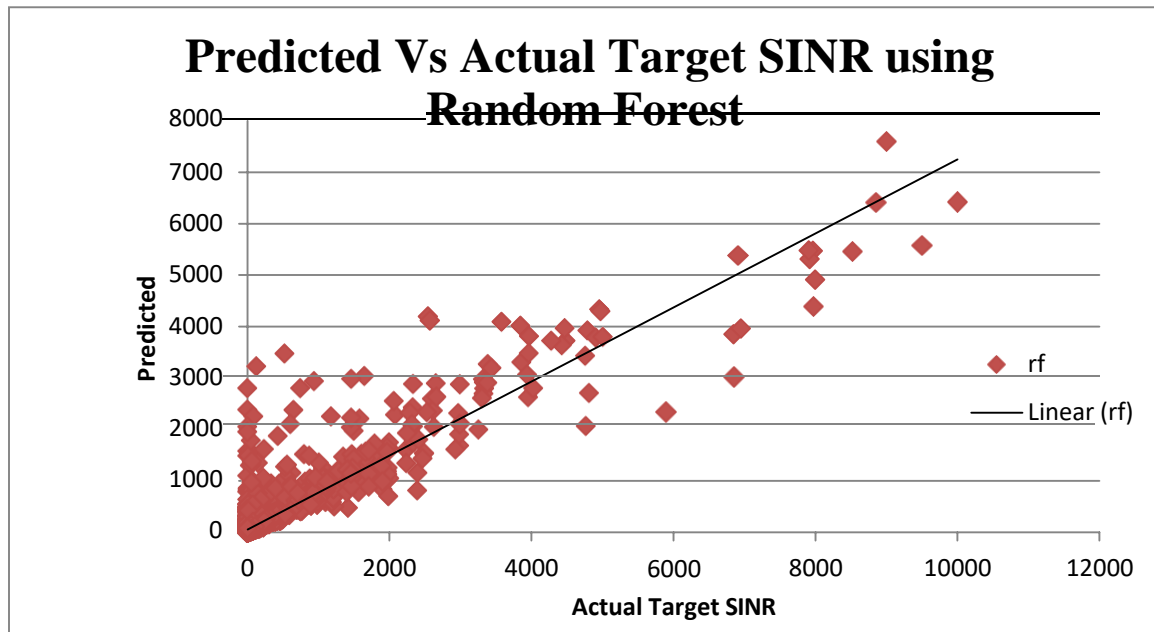
689 The 10-fold validation and cross-validation are used to measure the robustness of the RF model.
690 Fig. 7 depicts the scatter plot between true and predicted values of target SINR for 10 folds in the
691 validation experiment and this experiment is performed on 15% of the generated dataset. The
692 pseudo R-square value of 0.8675 from fig. 7 is very close to the pseudo R-square value of 0.8049
693 from fig. 6 (b). It makes sure that data set used is logical, complete and within acceptable limits.
694 Cross-validation result as shown in fig. 8 depicts the uniform performance on all evaluation
695 parameters of the model. This result is obtained by plotting the scatter plot between actual SINR
696 and predicted SINR of RF model and this plot resembles the validation scatter plot as shown in
697 fig. 7 to a much greater extent. It has been used to better estimate the test error of any model and
698 puts better confidence in the prediction accuracy of the model. It prevents the model over-fitting
699 and gives our model the opportunity to train on a number of train-test splits.

700
701



702
703
704
705
706

Fig. 7 Predicted vs. Observed in RF model during validation phase



730 **Fig. 8** Predicted vs. Observed in RF model during cross-validation phase

731
732 The observed SINR is plotted on the horizontal axis and predicted SINR on the vertical
733 axis of the scatter plot. The location of each point on the graph depends on both the
734 predicted and observed SINR values in figs. 5-8. The figs. 7 and 8 validate and cross-
735 validate the same conclusion-stronger; more linear and positive relationship between the
736 predicted and observed SINR values using the RF model as compared to the other three
737 ML models. The test set error is not utilized during the training phase. It is useful for
738 comparing various models and may be plotted during the training process. If it reaches a
739 minimum value than the validation set error for a particular iteration number, the data set
740 is poorly divided in nature. It is very difficult to know the speed of the employed training
741 algorithm, which depends upon various factors, such as the complexity of the problem,
742 the number of data points used in the training set, the number of control weights and
743 biases in the network, the target error, and whether the network is being utilized for
744 pattern recognition or function approximation.

5 Conclusion

BF is a noise mitigation scheme to improve the SINR ratio of received signals, and focus transmitted signals in desired spatial directions. The parameters of each path of multi-path propagation model are cleaved into the corresponding channel gain and the DOA information in the channel matrix. Here, the adaptive BF is used under low and high SINR regime using ML in MSINR sense. The ML models, namely Decision Tree, Random Forest, Linear Model and Neural Network are used to predict the target SINR responsible for BF. The optimization of antenna combining weights is based on MSINR value. The ML models are evaluated and compared in terms of performance analysis parameters, namely correlation, R^2 , Mean Absolute Error and % Accuracy on a data set generated using the python package pyArgus. Random Forest ML model is the best among the four ML models used and has the best performance analysis features as follows: Correlation-0.92, R^2 -0.85, Mean Absolute Error-70.73 and % Accuracy-86.40. The further research is required to improve the coding to enhance the performance analysis results shown in this paper. The proposed adaptive BF system may be applied in VSCs, which is to be explored in the next research. The more advanced antenna arrays can be used to overcome the optimum half-wavelength limit of arbitrary configured planar antenna systems.

REFERENCES

- [1] <https://github.com/zinka/arraytool> and <https://zinka.wordpress.com/>, S.R. Zinka, Python package.
- [2] Liu Z., J. He., "Linearly constrained minimum- 'normalised variance' beamforming against heavy-tailed impulsive noise of unknown statistics", IET Radar Sonar & Navigation, vol. 2, issue 6, pp. 449-57, 2008.

- 772 [3] Xiaotong Li, Ruiting Zhou, Ying-Jun Angela Zhang, Lei Jiao, Zongpeng Li, “Smart vehicular
773 communication via 5G mmWaves”, Elsevier, Computer Networks, vol. 172, pp. 1-12, 2020.
- 774 [4] Dian Fan, Feifei Gao, Yuanwei Liu, Yansha Deng, Gongpu Wang, Zhangdui Zhong, Arumugam
775 Nallanathan, “Angle Domain Channel Estimation in Hybrid mmWave Massive MIMO Systems”, IEEE
776 Trans. on Wireless Communications, pp. 1-15, 2018.
- 777 [5] Mietzner J., Schober R., Lampe L., Gerstacker W.H., Hoehner P.A., “Multiple Antenna Techniques for
778 Wireless Communication – a Comprehensive Literature Survey”, IEEE Commun. Surv. and Tutorials, vol.
779 11, no. 2, pp. 87–105, 2009.
- 780 [6] Dian Fan, Yansha Deng, Feifei Gao, Yuanwei Liu, Gongpu Wang, Zhangdui Zhong, Arumugam
781 Nallanathan, "Training Based DOA Estimation in Hybrid mmWave Massive MIMO Systems",
782 GLOBECOM 2017-2017 IEEE Global Commun. Conf., DOI: 10.1109/GLOCOM.2017.8254826, 2017.
- 783 [7] Fang X., W. Luo, M. Cheng, "Beamforming and Positioning-Assisted Handover Scheme for Long-
784 Term Evolution System in High-Speed Railway", IET Communications, pp. 2335-40, 2012.
- 785 [8] David Munoz, Frantz Bouchereau, Cesar Vargas, Rogerio Enriquez, “Book on Position Location
786 Techniques and Applications”, published by Elsevier, 2009.
- 787 [9] Balanis C. A., “Antenna Theory Analysis and Design”, John Wiley & Sons, New York, 1997.
- 788 [10] Krous J. D.: Antenna, Mc GRAW-HILL, New York, 1950.
- 789 [11] Ehab Ali, Mahamod Ismail, Rosdiadee Nordin, Nor Fadzilah Abdulah, “Review: Beamforming
790 Techniques for Massive MIMO Systems in 5G: Overview, Classification, and Trends for Future
791 Research”, Zhejiang University and Springer-Verlag Berlin Heidelberg, pp. 753-72, 2017.
- 792 [12] Anita V., Sri Jaya Lakshmi S., Sreedevi I., Khan H., Sarat Kumar K., Ramakrishna P., “An Adaptive
793 Processing of Linear Array for Target Detection Improve”, Int. J. Comput. Appl. (0975–8887), vol. 42, no.
794 4, pp. 33–6, 2012.
- 795 [13] Mailloux R. J., “Phased Array Architecture for Millimetric Active Arrays”, IEEE Antennas Propag.
796 Soc. Newslett., vol. 28, pp. 4–7, 1986.
- 797 [14] Schrank H. E., “Low Sidelobe Phased Array Antennas”, IEEE Antennas Propag. Soc. Newslett., vol.
798 25, no. 2, pp. 4–9, 1983.
- 799 [15] Applebaum S. P., Chapman D. J., “Adaptive Arrays with Main Beam Constraints”, IEEE Trans.
800 Antennas Propag., AI-24, pp. 650–62, 1976.
- 801
802
803
804
805
806
807
808
809

- 810 [16] Fangxiao Jin, Tianshuang Qiu, Tao Liu, “Robust Cyclic Beamforming against Cycle Frequency Error
811 in Gaussian and Impulsive Noise Environments”, *Int. J. Electron. Commun. by Elsevier*, pp. 153–60, 2019.
- 812 [17] Shepherd R. A., “Measurements of Amplitude Probability Distributions and Power of Automobile
813 Ignition Noise at HF”, *IEEE Trans. Veh. Technol.*, vol. 23, no. 3, pp. 72–83, 1974.
- 814 [18] Blackard K. L., Rappaport T. S., Bostian C. W., “Measurements and Models of Radio Frequency
815 Impulsive Noise for Indoor Wireless Communications”, *IEEE J. Sel. Areas Commun.*, pp. 991–1001, 1993.
- 816 [19] Tsakalides P., Nicias C. L., “Robust Space–time Adaptive Processing (STAP) in Non-Gaussian Clutter
817 Environments”, *IEE Proceedings-Radar, Sonar Navig.*, pp. 84–93, 1999.
- 818 [20] Kannan B., Fitzgerald W. J., “Beamforming in Additive A-Stable Noise using Fractional Lower Order
819 Statistics (FLOS)”, *Proc. IEEE Int. Conf. Electron. Circuits, Syst.*, pp. 1755–8, 1999.
- 820 [21] He J., Liu Z., Thomas Wong K., “Linearly Constrained Minimum- “Geometric Power” Adaptive
821 Beamforming using Logarithmic Moments of Data containing Heavy-Tailed Noise of Unknown Statistics”,
822 *IEEE Antennas Wirel. Propag. Lett.*, vol. 6, pp. 600–3, 2007.
- 823 [22] Zhao H., Zhang Y., Li E-P, Buonanno A., D’Urso M., “Diagnosis of Array Failure in Impulsive Noise
824 Environment using Unsupervised Support Vector Regression Method”, *IEEE Trans. Antennas Propag.*, vol.
825 61, no.11, pp. 5508–16, 2013.
- 826 [23] Ma W., Qu H., Gui G., Xu L., Zhao J., Chen B., “Maximum Correntropy Criterion based Sparse
827 Adaptive Filtering Algorithms for Robust Channel Estimation under Non-Gaussian Environments”, *J. of
828 the Franklin Institute*, pp. 2708–28, 2015.
- 829 [24] Chen B., Liu X., Zhao H., Principe J. C., “Maximum Correntropy Kalman Filter Automatica”, pp. 70–
830 7, 2017.
- 831 [25] Wu Z., Peng S., Chen B., Zhao H., “Robust Hammerstein Adaptive Filtering under Maximum
832 Correntropy Criterion”, *Entropy*, vol. 17, no. 12, pp. 7149–66, 2015.
- 833 [26] Hajiabadi M., Hodtani G.A., Khoshbin H., “Adaptive Multitask Network based on Maximum
834 Correntropy Learning Algorithm”, *Int. J. Adapt Control Signal Process.*, vol. 31, no. 8, pp. 1232–41, 2017.
- 835 [27] Chen B., Xing L., Zhao H., Zheng N., Principe J.C., “Generalized Correntropy for Robust Adaptive
836 Filtering”, *IEEE Trans. Signal Process.*, vol. 64, no. 13, pp. 3376–87, 2016.
- 837
838
839
840
841
842
843
844
845
846

- 847
848 [28] Taras Maksymyuk, Juraj Gazda, Oleh Yaremko, Denys Nevinskiy, "Deep Learning Based Massive
849 MIMO Beamforming for 5G Mobile Network", The 4th IEEE Int. Symposium on Wireless Systems, pp.
850 241-4, 2017.
- 851
852 [29] Vishnu V. Ratnam, Andreas F. Molisch, "Periodic Analog Channel Estimation Aided Beamforming
853 for Massive MIMO Systems", IEEE Transactions on Wireless Communications, vol. 18, no. 3, pp. 1581-
854 94, 2019.
- 855 [30] Kuo-Chen Ho, Shang-Ho Tsai, "A Novel Multiuser Beamforming System with Reduced Complexity
856 and Beam Optimizations", IEEE Transactions on Wireless Communications, vol. 18, no. 9, pp. 4544-57,
857 2019.
- 858 [31] Hang Li, Thomas Q. Wang, Xiaojing Huang, "Joint Adaptive AoA and Polarization Estimation using
859 Hybrid Dual-Polarized Antenna Arrays", IEEE Access, vol. 7, pp. 76353-66, 2019.
- 860 [32] Mohammed A. Almagboul, Feng Shu, Yaolu Qin, Xiaobo Zhou, Jin Wang, Yuwen Qian, Kingsley Jun
861 Zou, Abdeldime Mohamed Salih Abdelgader, "An Efficient Hybrid Beamforming Design for Massive
862 MIMO Receive Systems via SINR Maximization Based on an Improved Bat Algorithm", IEEE Access,
863 vol. 7, pp.136545-58, 2019.
- 864 [33] Hedi Khammari, Irfan Ahmed, Ghulam Bhatti, Masoud Alajmi, "Spatio-Radio Resource Management
865 and Hybrid Beamforming for Limited Feedback Massive MIMO Systems", J. of Electronics,
866 DOI:10.3390/electronics8101061, pp. 1-25, 2019.
- 867 [34] Ahmet M. Elbir, "CNN-Based Precoder and Combiner Design in mmWave MIMO Systems", IEEE
868 Communications Letters, vol. 23, no. 7, pp. 1240-43, 2019.
- 869
870 [35] Lorenzo Combi, Umberto Spagnolini, "Adaptive Optical Processing for Wideband Hybrid
871 Beamforming", IEEE Transactions on Communications, vol. 67, no. 7, pp. 4967-79. 2019.
- 872 [36] Susnata Mondal, Jeyanandh Paramesh, "A Reconfigurable 28-/37-GHz MMSE-Adaptive Hybrid-
873 Beamforming Receiver for Carrier Aggregation and Multi-Standard MIMO Communication", IEEE
874 Journal of Solid-State Circuits, vol. 54, no. 5, pp. 1391-406, 2019.
- 875 [37] Linlin Sun, Yaolu Qin, Zhihong Zhuang, Riqing Chen, Yijin Zhang, Jinhui Lu, Feng Shu, Jiangzhou
876 Wang, "A Robust Secure Hybrid Analog and Digital Receive Beamforming Scheme for Efficient
877 Interference Reduction", IEEE Access, vol. 7, pp. 22227-34, 2019.
- 878
879 [38] Li Zhu, Shilian Wang, Jiang Zhu, "Adaptive Beamforming Design for Millimeter-Wave Line-of-Sight
880 MIMO Channel", IEEE Communications Letters, vol. 23, no. 11, pp. 2095-98, 2019.

- 881 [39] Yanan Liu , Xianbin Wang , Gary Boudreau , Akram Bin Sediq, Hatem Abou-zeid, “Deep Learning
882 Based Hotspot Prediction and Beam Management for Adaptive Virtual Small Cell in 5G Networks”, IEEE
883 Transactions on Emerging Topics in Computational Intelligence, vol. 4, no. 1, pp. 83-94, 2020.
- 884 [40] Song Noh, Michael D. Zoltowski, David J. Love, “Multi-Resolution Codebook and Adaptive
885 Beamforming Sequence Design for Millimeter Wave Beam Alignment”, IEEE Transactions on Wireless
886 Communications, vol. 16, no. 9, pp. 5689-501, 2017.
- 887 [41] Shi Q., Razaviyayn M., Luo Z.Q., and He C., “An Iteratively Weighted MMSE Approach to
888 Distributed Sum-Utility Maximization for a MIMO Interfering Broadcast Channel,” IEEE Trans. Signal
889 Process., vol. 59, no. 9, pp. 4331-40, 2011.
- 892 [42] Yaohua Sun, Mugen Peng, Yangcheng Zhou, Yuzhe Huang, Shiwen Mao, “Application of Machine
893 Learning in Wireless Networks: Key Techniques and Open Issues”, IEEE Commun. Surv. and Tutorials,
894 pp.1-37, 2019.
- 895 [43] Mingyi Hong, Zhi-Quan Luo, "Joint Linear Precoder Optimization and Base Station Selection for an
896 Uplink MIMO Network: a Game Theoretic Approach", 2012 IEEE Int. Conf. on Acoustics, Speech and
897 Signal Processing (ICASSP), pp. 2941-44, 2012.
- 898 [44] Bjornson E., Bengtsson M., Ottersten B., “Optimal Multiuser Transmit Beamforming: A Difficult
899 Problem with A Simple Solution Structure,” IEEE Signal Processing Magazine, vol. 31, no. 4, pp. 142–8,
900 2014.
- 901 [45] Balanis C. A., “Antenna Theory: Analysis and Design”, 3rd ed.; Wiley-Interscience: New York, NY,
902 USA, 2005.
- 903 [46] Monzingo R. A., Miller, T. W., “Introduction to Adaptive Arrays”, Scitech. Publishing Inc.: Raleigh,
904 NC, USA, 2004.
- 905 [47] Haykin S., “Adaptive Filter Theory”, 3rd ed.; Prentice Hall: Upper Saddle River, NJ, USA, 1996.
- 906 [48] Abhinav Sharma, Sanjay Mathur, “Performance Analysis of Adaptive Array Signal Processing
907 Algorithms”, IETE Technical Review, pp. 1-20, DOI: 10.1080/02564602.2015.1088411, 2016.
- 908 [49] Quinlan J. R., “Induction of Decision Trees”, Machine learning, vol. 1, no. 1, pp. 81–106, 1986.
- 909
- 910
- 911
- 912
- 913
- 914
- 915
- 916
- 917

- 918 [50] Liaw A, Wiener M., "Classification and Regression by Random Forest", R News, vol. 2/3: pp.18–22,
919 2002.
- 920 [51] Chambers J. M., "Computational Methods for Data Analysis", Applied Stat., vol. 1, no. 2, pp.1–10,
921 1977.
- 922 [52] Riedmiller M., Braun H., "A Direct Adaptive Method for Faster Backpropagation Learning: The
923 RPROP algorithm", IEEE Int. Conf. on Neural Nets, pp. 586–91, 1993.
- 924 [53] Prashant Singh Rana, Harish Sharma, Mahua Bhattacharya, Anupam Shukla. "Quality assessment of
925 modeled protein structure using physicochemical properties", Journal of Bioinformatics and Computational
926 Biology, vol. 13, no. 2, pp. 1-19, 2015.
- 927 [54] Francisco Hugo Costa Neto Daniel Costa Araújo Tarcisio Ferreira Maciel, "Hybrid beamforming
928 design based on unsupervised machine learning for millimeter wave systems", John Wiley & Sons, Ltd.,
929 pp. 1-18, 2020.
- 930 [55] Hyung Jun Kwon, Jung Hoon Lee, and Wan Choi, "Machine Learning-Based Beamforming in Two-
931 User MISO Interference Channels", ICAIIC, IEEE, pp. 496-99, 2019.
- 932
933
934
935

936 Authors



937 **Sanjeev Chopra** received his B.E. degree in Electronics and Instrumentation Engineering from
938 Punjabi University, Punjab, India in 1997; M. Tech. degree in Electronics and Communication
939 Engineering from Punjab Technical University, Punjab, India in 2010. He has twenty years'
940 teaching experience from July 1997 to July 2017. He has published 12 research papers in
941 various reputed Journals and Conferences. He is presently a Ph.D. scholar in Electronics and
942 Communication Engineering Department of Thapar Institute of Engineering and Technology, Patiala,
943 Punjab, India. His research areas are Wireless Communication, Image Processing and Biomedical
944 Electronics.



945 **Dr. Ajay Kakkar** is presently working as Assistant Professor in the ECED of T.I.E.T., Patiala,
946 Punjab, India. He has done his B. Tech., M.E. and Ph.D. in 1998, 2002 and 2013 respectively. He
947 has also completed one-year program "New-Directions in Teaching & Learning" in distinction, the
948 course was jointly organized by Thapar University, Patiala and TCD, Ireland. He has more than 13
949 years of teaching experience. He has chaired sessions in various conferences/workshops organized by
950
951
952
953
954
955

different agencies. He has also published more than 30 research papers in various Conferences/Journals which include IEEE, Elsevier, Taylor and Francis. His research interests include Image and Data Security, Adhoc Networks, and Renewable and Sustainable energy.